Global Biogeochemical Cycles

RESEARCH ARTICLE
10.1029/2017GB005634

Key Points:
- We estimated net community production (NCP) by summing the mixed layer reduction in dissolved inorganic carbon in N-depleted ocean gyres
- The mixed layer C_T reduction was calculated from an annual C_T cycle, deduced from global records of surface pCO_2 and total alkalinity
- Our study suggests that N_2 fixation by microorganisms is a major driver for this NCP in the vast areas of ocean gyres

Supporting Information:
- Supporting Information S1
- Data Set S1
- Data Set S2

Correspondence to:
K. Lee,
ktl@postech.ac.kr

Citation:
Ko, Y. H., Lee, K., Takahashi, T., Karl, D. M., Kang, S.-H., & Lee, E. (2018). Carbon-based estimate of nitrogen fixation-derived net community production in N-depleted ocean gyres. *Global Biogeochemical Cycles*, *32*. https://doi.org/10.1029/2017GB005634

Received 31 JAN 2017
Accepted 21 JUL 2018
Accepted article online 30 JUL 2018

©2018. American Geophysical Union. All Rights Reserved.

Carbon-Based Estimate of Nitrogen Fixation-Derived Net Community Production in N-Depleted Ocean Gyres

Young Ho Ko[1], Kitack Lee[1], Taro Takahashi[2], David M. Karl[3], Sung-Ho Kang[4], and Eunil Lee[5]

[1]Division of Environmental Science and Engineering, Pohang University of Science and Technology, Pohang, South Korea, [2]Lamont-Doherty Earth Observatory of Columbia University, Palisades, NY, USA, [3]Daniel K. Inouye Center for Microbial Oceanography: Research and Education, University of Hawai'i at Mānoa, Honolulu, HI, USA, [4]Division of Polar Ocean Sciences, Korea Polar Research Institute, KIOST, Incheon, South Korea, [5]Ocean Research Division, Korea Hydrographic and Oceanographic Agency, Busan, South Korea

Abstract Accurate estimation of net community production (NCP) in the ocean is important for determining the future trend for carbon dioxide concentrations in the atmosphere and thus for understanding the global carbon cycle and climate change. Most methods for measuring NCP rely on analysis of dissolved fixed inorganic nitrogen species (N), which are believed to be limiting factors for NCP. However, in the vast areas of the ocean gyres only low levels of N are available for phytoplankton during much of the year. In this study the NCP was estimated by summing the seasonal reduction in the concentration of dissolved inorganic carbon (C_T) in the surface mixed layer, corrected for changes associated with salinity variation, net air-sea CO_2 flux, horizontal C advection, non-Redfield diffusive C and N fluxes (deviations from the C:N ratio of 7), and anthropogenic nitrogen deposition. The mixed layer reduction in C_T was calculated from an annual C_T cycle, deduced from comprehensive records of surface pCO_2 and total alkalinity, using an established thermodynamic model. This method yielded a value of 0.6 ± 0.2 Pg of C, which represents the NCP that occurred during the warming period (approximately 8 months) in the nitrate-depleted (<0.2 μmol/kg) ocean. Our estimate is broadly consistent with the global N_2 fixation rate estimated using the ^{15}N-based method and suggests that N_2 fixation by microorganisms is a major driver for this NCP.

1. Introduction

Dissolved forms of fixed inorganic nitrogen (nitrate, NO_3^-; nitrite; and ammonium: hereafter referred to as N) are indispensable nutrients for marine life and largely determine the phytoplankton biomass throughout much of the global ocean. However, the concentrations of N are low in subtropical ocean gyres, as the sunlit upper layers are permanently stratified and vertical transport (via diffusion and advection) of N from deep waters to the sunlit layers is limited. As a result of low concentrations of N in surface waters of the ocean gyres, new photosynthetic production depends on external (as opposed to recycled) supply of nutrients. In the oligotrophic ocean, N limitation is ameliorated by a diverse assemblage of diazotrophs, which reduce strongly bonded N_2 to ammonia and dissolved organic nitrogen (DON) via an energy intensive process of N_2 fixation (Capone et al., 1997; Karl et al., 2002). This process is known to be a major source of N to the oligotrophic ocean, accounting for approximately 50% of the total external source of N (Galloway et al., 2004; Gruber & Galloway, 2008; Raes et al., 2015).

Despite the potential importance of N_2 fixation in regulating phytoplankton biomass and net community production (NCP) in the oligotrophic ocean, the global rate of N_2 fixation has remained poorly constrained. This is because shipboard measurements based on the acetylene reduction assay or the $^{15}N_2$ assimilation have not been able to resolve the temporal and spatial dynamics of N_2 fixation. Another impediment to obtaining accurate estimates is that these two methods yield different rates of N_2 assimilation into the biomass. This large difference in rate is inevitable because the acetylene method provides an indirect estimate of gross N_2 fixation whereas the ^{15}N tracer method measures the net rate of ^{15}N assimilation (Böttjer et al., 2017; Mulholland, 2007; Wilson et al., 2012). Approximately 60% of the measured rates reported to date have been based on the $^{15}N_2$ assimilation method (Luo et al., 2012). Moreover, the ^{15}N-based rates reported earlier are a factor of 2 or more lower than recent measurements, because the earlier measurements were subject to the problem of incomplete equilibrium of $^{15}N_2$ gas with the seawater sample (Böttjer et al., 2017; Großkopf et al., 2012). Assessment of ^{15}N isotope abundance in sinking organic matter is an alternative to ^{15}N-

labeled incubation methods for estimating the relative contributions of N sources supporting new production. However, data obtained using this method are not sufficient to provide a global estimate. More importantly, the accuracy of this method relies on several key assumptions, including a steady state condition, a low level of export of DON, and an accurate estimate of the ^{15}N content of the nitrate transported to the upper ocean, all of which need to be confirmed (Böttjer et al., 2017; Gruber, 2016).

Alternative methods based on biogeochemical models and geochemical tracers (e.g., N^* and P^*) have been used to estimate regional and global rates of N_2 fixation (Deutsch et al., 2007; Gruber & Sarmiento, 1997), but as these are indirect methods so the model predictions need field verification. For example, the N_2 fixation rate estimated from the excess of NO_3^- in seawater compared with that predicted using measured phosphate (PO_4^{3-}; $N^* = NO_3^- - 16 \times PO_4^{3-}$) relies on the elemental N:P ratio of organic matter produced by N_2 fixing organisms and those that do not fix N_2. However, reported N:P ratios of organic matter vary greatly, primarily because elemental stoichiometry depends on taxonomic composition and accumulated detritus; these factors make the estimation of the N_2 fixation rate from N^* signals unreliable (Martiny et al., 2013). Moreover, the N^* signal reflects the net effect of N_2 fixation and denitrification and is affected by anthropogenic N that has entered the ocean via atmospheric deposition (Duce et al., 2008; T.-W. Kim et al., 2011; I.-N. Kim et al., 2014). Another indirect method is based on seawater P^* ($P^* = PO_4^{3-} - NO_3^-/16$) or P_T^* ($P_T^* = [PO_4^{3-} + DOP] - [NO_3^- + DON]/16$) signals (Deutsch et al., 2007). This method assumes that N_2 fixation activity is more closely associated with sources of elevated P^*, probably caused by denitrification in the water column. Therefore, it calculates the difference between surface P^* values and those predicted from upwelled P^*, with the difference attributed to N_2 fixation activity. However, it involves the same errors that influence the N^*-based method. Therefore, substantial differences in estimates of the N_2 fixation rate based on direct and indirect methods are inevitable.

To overcome the problems inherent in the N_2 fixation measurement methods (direct or indirect) that require conversion of N_2 fixation to NCP, we directly estimated the seasonal reduction of dissolved inorganic carbon ($C_T = [HCO_3^-] + [CO_3^{2-}] + [CO_2]$) in the mixed layer during the period of N depletion. A reduction in the concentration of C_T in the absence of N was first reported at the Bermuda Atlantic Time-series Study (BATS; 31°N, 64°W, http://bats.bios.edu/; Michaels et al., 1994) and the Hawaii Ocean Time-series (HOT; 23°N, 158°W, http://hahana.soest.hawaii.edu/hot/hot-dogs/) stations (Karl et al., 2003). Subsequently, by applying the empirical algorithms between salinity (S)-normalized C_T ($nC_T = C_T \times 35/S$) and sea surface temperature (SST) derived from a small C_T data set ($n \sim 16{,}000$) to the global ocean, Lee et al. (2002) inferred that this phenomenon could be widespread throughout tropical and subtropical oceans. The major limitation of the study of Lee et al. (2002) was its reliance on a restricted C_T data set that poorly resolved the seasonal evolution of C_T in the world ocean.

In the present study, we used large data sets of seawater pCO_2 comprising approximately 6.5 million data, which are 2 orders of magnitude greater than the C_T data set; this enabled accurate resolution of the seasonal evolution of pCO_2 in much of the world oceans. In particular, the combination of this data set with a surface alkalinity data set (Lee et al., 2006) and the established thermodynamic model for the seawater carbonate system should enable the seasonal evolution of C_T in the world oceans to be accurately resolved. We describe here a novel method for estimating NCP values in waters containing depleted levels of N, based on the mixed layer nC_T reduction. The NCP estimate could be attributed only to N_2 fixation (NCP_{N2fix}). The values for NCP_{N2fix} determined in N-depleted waters were compared with literature values inferred from various estimates of N_2 fixation rates.

2. Computation Methods

In the oligotrophic ocean, we estimated the rate of NCP_{N2fix} from reductions in the nC_T inventory within the mixed layer and corrected for changes arising from the net air-sea CO_2 flux, horizontal C advection, the diffusive C_T and NO_3^- flux, and the atmospheric deposition of pollutant N. To achieve this, we used the following equation:

$$NCP_{N2fix} = \left(AH\left[nC_T^M - nC_T^{M+1}\right]\right) + AF_{AIR\text{-}SEA} - Au(dnC_T/dx) + AK_v[dC_T/dm - (C/N)dN/dm] - A(C/N)AND \quad (1)$$

where A (m^2) is the area of each pixel (4° latitude × 5° longitude); M is the time step (months); $[nC_T^M - nC_T^{M+1}]$ is the decrease in the nC_T concentration at the mean mixed layer depth

($H = [H^M + H^{M+1}]/2$) over consecutive months; F (mol·m^{-2}·month^{-1}) is the net air-sea CO_2 flux; u is the mean horizontal advective velocity (m/s), and dnC_T/dx is the mean horizontal gradient of nC_T; K_V (m^2/month) is the eddy diffusivity across the bottom of the mixed layer; and dC_T/dm and dN/dm (mol m^{-4}) are the vertical gradients of C_T and NO_3^- concentrations in the upper thermocline, respectively. AND is the atmospheric deposition of pollutant N (mol·m^{-2}·month^{-1}). Equation (1) was applied only when the mixed layer nC_T concentration decreased over several months of the year (approximately consistent with the period of warming) and only for pixels in which the mean NO_3^- concentration remained <0.2 μmol/kg. This cutoff point for the NO_3^- concentration was used because marine cyanobacteria of the genus *Trichodesmium*, which is a cosmopolitan N_2 fixing microorganism, mostly occur in waters where the NO_3^- concentration is <0.2 μmol/kg (Hood et al., 2004, 2000).

For each pixel, the annual cycle of the mixed layer C_T concentration was calculated from monthly mean pCO_2 and A_T data using the carbonic acid dissociation constants of Mehrbach et al. (1973; with the functional forms refitted by Dickson & Millero, 1987), other auxiliary thermodynamic constants (including the solubility of CO_2; Weiss, 1974; and the dissociation constants for boric acid; Dickson, 1990, and phosphoric acid; Yao & Millero, 1995), and the total boron concentration estimated by Lee et al. (2010). This set of thermodynamic constants was consistent with both laboratory and field data (Lee et al., 1996, 2000). Seawater pCO_2 data collected over a 55-year time span (1957–2012) were normalized to each month of the reference year of 2005 by accounting for oceanic uptake of anthropogenic CO_2 (Takahashi et al., 2014). The estimated monthly mean pCO_2 values for the year 2005 are available at https://www.nodc.noaa.gov/ocads/oceans/ndp_094/ndp094.html. Monthly mean values of A_T were estimated from the A_T–SSS-SST algorithms (Lee et al., 2006) and monthly records of SSS and SST. Monthly mean SSS and SST data are obtained from the World Ocean Atlas 2009 (Antonov et al., 2010; http://www.nodc.noaa.gov/OC5/WOA09/woa09data.html) and National Centers for Environmental Prediction Reanalysis data (https://www.esrl.noaa.gov/psd/data/reanalysis/reanalysis.shtml), respectively. We removed variations in C_T associated with salinity variations (due to evaporation/precipitation) by normalizing C_T values to a mean salinity ($\bar{S}$) representing the warming period using $nC_T = C_T \times \bar{S}/S$, where S is the monthly mean salinity. To calculate the mixed layer reduction in nC_T, a linear regression was applied to nC_T data obtained for the selected warming periods. To minimize biases caused by questionable data, we used a traditional mean and standard deviation method to remove those data points. Thus, during fitting of the data we excluded all nC_T values having residuals (measured values minus those predicted) that exceeded 2 standard deviations from the mean residual value.

To integrate the mixed layer nC_T reduction during the warming period, we used records of monthly mean mixed layer depth derived using the −0.2 °C vertical temperature gradient (de Boyer Montégut et al., 2004; http://www.ifremer.fr/cerweb/deboyer/mld/Surface _Mixed_Layer_Depth.php). Climatological (time-independent) monthly mean surface NO_3^- data from the World Ocean Atlas 2013 Version 2 (Garcia et al., 2014; https://www.nodc.noaa.gov/OC5/woa13/) were used to evaluate whether a given pixel had a NO_3^- concentration < 0.2 μmol/kg. These climatological NO_3^- data are heavily skewed to the earlier periods (1980s–1990s), whereas the pCO_2 climatological data are skewed to more recent periods (2000s onward). This apparent mismatch could lead to underestimation of the areal extent of N-depleted ocean (for which we had estimated NCP_{N2fix} values), if the N-depleted subtropical gyres have increased over time between these two periods during which most NO_3^- and pCO_2 data are available (1980s–1990s for NO_3^- vs, 2000s onward for pCO_2). However, the observation of no significant trend of change in the NO_3^- concentrations found in the HOT and BATS stations (Kavanaugh et al., 2018; Lomas et al., 2013) and in the extended study area (e.g., North Pacific Ocean; Yasunaka et al., 2016) suggests that this climatological NO_3^- field is representative of the period from 2000 onward.

Following the procedure described by Takahashi et al. (2009), monthly mean net air-sea CO_2 fluxes were estimated using the climatological seawater pCO_2 field (Takahashi et al., 2014), atmospheric pCO_2 data for 2005, the air-sea gas transfer rate, and the solubility of CO_2 in seawater (Weiss, 1974; see supporting information).

Horizontal advective transports impact the seasonal nC_T cycle (and therefore the magnitude of nC_T reduction). The rate of horizontal nC_T transport between the analysis pixels was estimated using the horizontal nC_T gradient and the current velocity during the warming period. The zonal and meridional gradients in nC_T were estimated from the nC_T field, calculated from climatological pCO_2 and A_T data. Zonal and meridional flows were estimated from the monthly climatological current field computed for the period 1993–2017

using the Geostropic and Ekman Current Observatory product (Sudre et al., 2013), in which geostrophic and Ekman velocities were estimated from the combination of satellite altimetry and scatterometer wind stress data.

The flux of C_T and NO_3^- from the upper thermocline into the mixed layer via eddy diffusion could either increase or decrease the mixed layer reduction in nC_T resulting from NCP_{N2fix} depending on whether the ratio of the fluxes of C_T and NO_3^- from the upper thermocline was less than or greater than 7, respectively. Specifically, if the flux ratio of C_T and NO_3^- into the mixed layer is greater than 7 (indicating that the flux of C_T is in excess relative to that of NO_3^-), the excess C_T would offset the nC_T reduction. The monthly fluxes of C_T and NO_3^- into each pixel via eddy diffusion were calculated using a basin-scale vertical gradient (Table S1 in the supporting information) of C_T and NO_3^- representing the given pixel and eddy diffusivity, K_V of 0.2–0.3 cm^2/s representing the upper thermocline of a subtropical ocean (Kim et al., 2005; Ledwell et al., 1998). Vertical C_T and NO_3^- data were obtained from the Global Ocean Data Analysis Project Version 2 (Olsen et al., 2016; https://www.nodc.noaa.gov/ocads/oceans/GLODAPv2/). The mixed layer reduction in nC_T was then corrected for the C_T difference in the ratio of C_T flux and that calculated using the concurrent flux of NO_3^- multiplied by a C:N ratio of 7 (Table S1). During the warming period, the mixed layer generally shoals but intermittent entrainment (e.g., caused by eddies and storms) also occurs due to short periods of wind-induced mixed layer deepening (McGillicuddy et al., 2007; Zhang et al., 2001). The effect of the entrainment process on the mixed layer nC_T budget would be similar to that of the diffusive flux. However, its influence is probably insignificant, given that the evolution of mixed layer temperature can be accurately predicted without accounting for entrainment (Gruber et al., 1998).

The NCP contributed by AND was estimated by multiplying the rate of atmospheric N deposition by a C:N ratio of 7. The rate of AND was obtained from multimodel global data sets of atmospheric N deposition, simulated particularly for the year 2000 (Lamarque et al., 2013; http://data.ceda.ac.uk/badc/accmip/data/GISS/).

3. Results and Error Analysis

In the widespread areas of the tropical and subtropical oceans the surface nC_T concentration decreased during the period of N depletion, which started in early spring and extended to late fall. The rate of nC_T decrease differed spatially, but the general trend among the oceans examined indicated a strong inverse correlation between nC_T and SST during the warming period (Figure 1). The accuracies of the estimated nC_T reductions were assessed by comparing the nC_T reductions measured for periods spanning 24–26 years at the BATS and the HOT stations against the estimates for those pixels encompassing these time-series stations. The NCP_{N2fix} values (0.9 ± 0.2 mol C/m^2 per 8 months at HOT and 1.7 ± 0.3 mol C/m^2 per 8 months at BATS) estimated using time-series data were consistent with values based on pCO_{2SW} and A_T data (1.0 ± 0.2 mol C/m^2 per 8 months and 1.5 ± 0.2 mol C/m^2 per 8 months, respectively), which were determined from pixels that include the HOT and BATS stations (Figure 2). This is a strong indication that the proposed method can accurately reproduce the seasonal evolution of surface C_T and its total reduction. Note that the AND contributions to the seasonal nC_T reductions at the BATS and HOT stations were relatively small (<10% at BATS and <5% at HOT).

When individual estimates (Data Set S1) for all pixels in which the mixed layer nC_T reduction occurred in the absence of N were integrated globally, the results yielded NCP_{N2fix} of 0.6 ± 0.2 Pg C per 8 months (Pg = petagrams = 10^{15} grams; Figure 3) after corrections were made for changes arising from net air-sea CO_2 flux (0.03 Pg C per 8 months), horizontal C_T flux (0.15 Pg C per 8 months), diffusive C_T (0.09 Pg C per 8 months) and NO_3^- (0.09 Pg C per 8 months) fluxes, and atmospheric N deposition (0.05 Pg C per 8 months; Tables S1 and S2).

Regional values of NCP_{N2fix} differed distinctly among latitudinal bands (Figure 3). Values for the latitude bands of 20–30°N and 20–30°S appeared to be higher than that for the lower latitude band of 20°N–20°S. It is important to note that seasonal nC_T drawdown in N-rich areas outside of the study area is considerably greater than that observed in the N-depleted region. For example, the NCP integrated for all areas except the N-depleted region was estimated to be 6.6 Pg C per 8 months, which is consistent with the range (5.9–7.2 Pg C per 8 months) reported by Lee (2001), based on the seasonal cycle of nC_T concentrations derived from monthly mean pCO_2 and A_T data, and regional nC_T relationships (Lee et al., 2000).

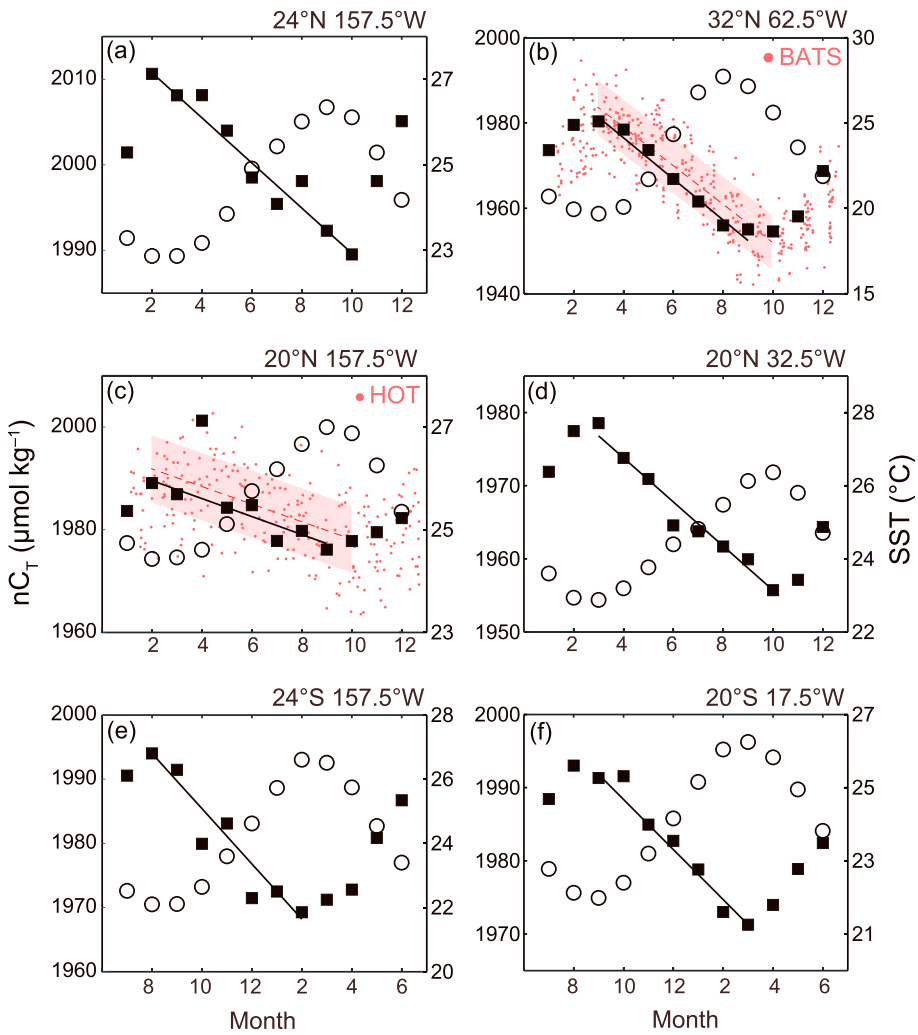

Figure 1. Examples of monthly mean values of nC_T (filled squares) and SST (open circles) for pixels (4° × 5°) in our analysis. The black solid lines show the linear regression lines for the nC_T decrease during the warming period. The red dots represent measured nC_T values at the BATS (b) and the HOT (c) stations, which are normalized to a single reference year (2005) using the linear regression trend of 1.55 ± 0.12 μmol·kg^{-1}·year^{-1} for BATS and 1.75 ± 0.13 μmol·kg^{-1}·year^{-1} for HOT. The black solid lines show the linear regression lines for the measured nC_T decrease and the red shaded areas represent the estimated uncertainty (1σ). SST = sea surface temperature; BATS = Bermuda Atlantic Time-series Study; HOT = Hawaii Ocean Time-series.

The effect of horizontal nC_T transport on estimates of the nC_T drawdown in each pixel depended on the sign and magnitude of the horizontal C_T gradient and current velocities (Figure S1). In the subtropical gyres of the North and South Pacific Ocean, the horizontal nC_T transport increased the seasonal nC_T drawdown because of the poleward increase in nC_T and the poleward surface current. However, our NCP_{N2fix} values are underestimated for areas between 12°N and 24°N in the Atlantic Ocean, where both the eastward increase in the nC_T gradient and the westward surface current decreased the seasonal nC_T drawdown. The net horizontal nC_T transport in all basins for which NCP_{N2fix} values are available was estimated to be in the range −0.04 to 0.13 Pg C per 8 months (Table S2).

NCP_{N2fix} values are not sensitive to the addition of NO_3^- via entrainment of subsurface waters and eddy diffusion. In oligotrophic oceans, NO_3^- transported into the euphotic layer is completely utilized along with C_T at the Redfield C:N ratio of 7. Therefore, the NCP_{N2fix} value, which is determined based on changes in C_T in NO_3^- depleted waters, would be affected only by the small residual C_T resulting from deviations in the C:N ratio in upwelled water. The diffusive C_T flux could have decreased our local and global NCP_{N2fix} estimates,

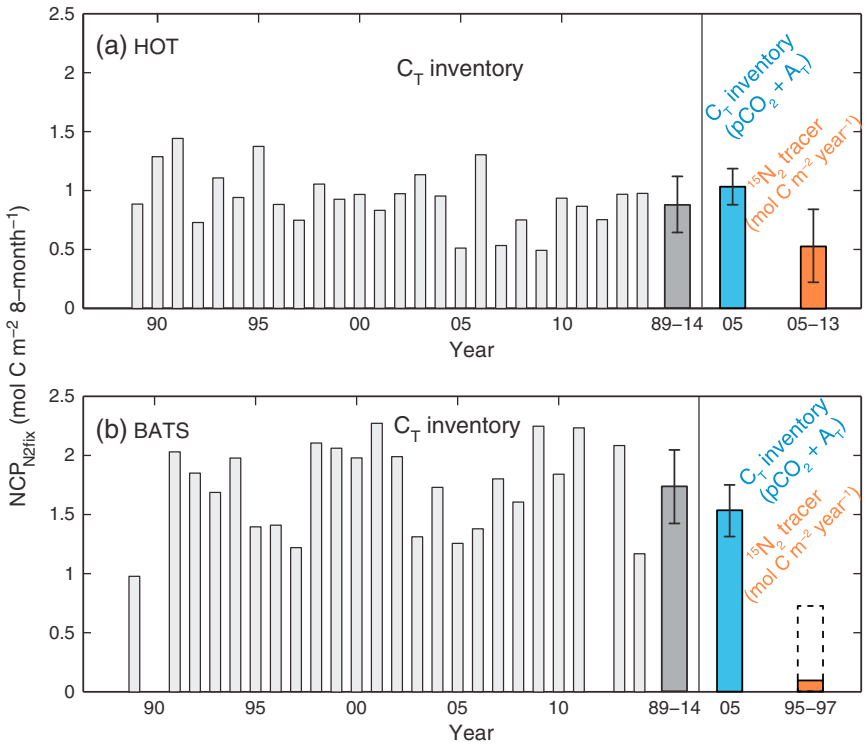

Figure 2. Estimates of NCP_{N2fix} from integration of seasonal nC_T reductions observed at the (a) HOT and (b) BATS stations. NCP_{N2fix} values averaged over 26 and 24 years at the HOT and the BATS stations, respectively, were compared with the estimates for those pixels including the BATS and the HOT stations and with those based on field N_2 fixation-based measurements (Böttjer et al., 2017; Orcutt et al., 2001). The dashed bar for the (b) BATS station indicates the revised rate obtained after correcting for errors associated with incomplete $^{15}N_2$ equilibrium and assessments of the abundance of N_2 fixing organisms. The revised rate is a factor of 8 greater than the reported rate at the BATS station. HOT = Hawaii Ocean Time-series; BATS = Bermuda Atlantic Time-series Study; NCP = net community production.

whereas the diffusive NO_3^- flux could have increased our NCP_{N2fix} estimates. However, their combined contributions to the global NCP_{N2fix} estimate were negligible (<1%), because the C:N ratios of diffusive C_T and NO_3^- fluxes from the upper thermocline were close to the Redfield ratio of 7 throughout most of our

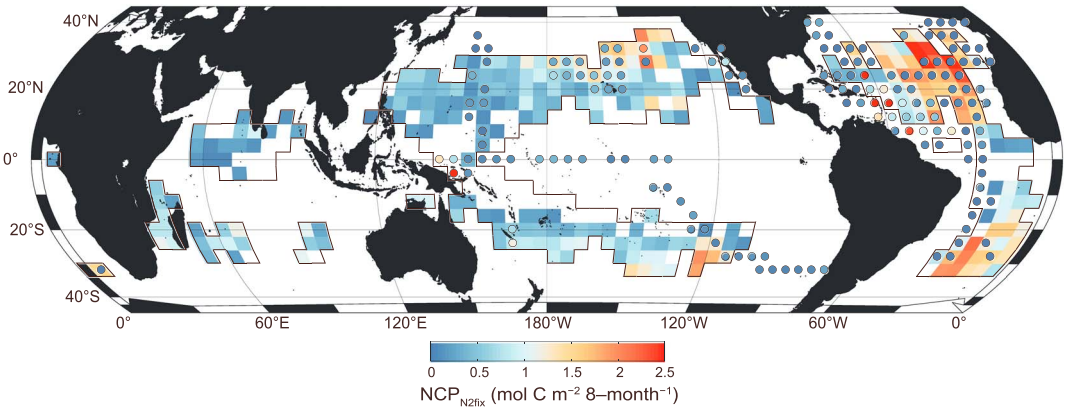

Figure 3. NCP_{N2fix} in N-depleted waters (NO_3^- concentrations <0.2 μmol/kg are indicated as black solid boxes). White pixels within the solid boxes indicate no C_T drawdown during the warming period. NCP_{N2fix} values are expressed as mol C/m^2 for 8-month warming season. The integrated NCP_{N2fix} calculated using equation (1) was 0.6 ± 0.2 Pg C per 8 months. The colored circles show gridded synthesis of N_2-supported NCP calculated from direct measurements of N_2-fixation rates (data from Luo et al. (2012; https://doi.org/10.1594/PANGAEA.774851). NCP = net community production.

study area (Table S1). The N contribution via episodic N input from depth associated with mesoscale eddies cannot be accurately estimated because of inadequate knowledge of this diffusive flux in terms of location and time (Pidcock et al., 2016). One way of estimating this effect is to perform a sensitivity analysis by varying the K_V value, because eddies are known to enhance vertical diffusivity (McGillicuddy et al., 1998). The diffusivity-driven NCP ranged from 0.003 to 0.014 mol C per 8 months when the K_V was varied from 0.1 to 0.5 cm^2/s; this has only minor impact on our NCP_{N2fix} estimates.

Atmospheric N deposition would increase our estimate, but its influence was largely confined to areas north of the N-depleted subtropical and tropical oceans (Lamarque et al., 2013), where our estimate was almost 0. As a result, the contribution of atmospheric N deposition to the estimated NCP_{N2fix} for the ocean areas where C_T removal in the absence of N occurred concurrently was only 0.05 Pg C per 8 months.

Our estimate of NCP_{N2fix} may be affected by errors in estimates of the mixed layer nC_T fields, the mixed layer depth, horizontal C_T flux and the net air-sea CO_2 flux. The fits between nC_T and month for all the pixels had a mean uncertainty of ±15%, which led to an uncertainty of ±0.1 Pg C per 8 months in our estimate. The mean difference in the mixed layer depth calculated using two independent criteria (the water depth at which vertical gradients in density and temperature become $\Delta\sigma_\theta = 0.03$ kg/m^3 and $\Delta t = 0.2$ °C, respectively) resulted in a difference of ±0.1 Pg C per 8 months. Uncertainty associated with the horizontal C_T flux depends on uncertainties about current velocities (assumed to be ±50% error, based on Quay & Stutsman, 2003) and the horizontal nC_T gradient among pixels (±25%, estimated in this study from the fit between nC_T and latitude or longitude). In combination, these uncertainties accounted for a difference of ±0.06 Pg C per 8 months in our global NCP_{N2fix} estimate.

The uncertainty in estimation of the net air-sea CO_2 flux resulted in a difference of ±0.03 Pg C per 8 months, depending on the choice of parameterizations between the gas exchange rate and the wind speed. In producing the pCO_2 climatology used in our analysis to estimate nC_T, Takahashi et al. (2009) used a 2-D lateral transport model to account for the effect of the lateral transport of water on pCO_2 interpolation for each pixel. This effect led to a systematic bias of +1.3 μatm of the interpolated pCO_2 and thereby an error of 0.04 Pg C per 8 months in our estimate of net air-sea CO_2 flux, which is equivalent to 5% of our NCP_{N2fix} estimates. Our value (0.03 Pg C per 8 months) of net air-sea CO_2 flux includes correction for systematic bias of interpolated pCO_2 value. One outstanding issue in error estimates associated with the net air-sea CO_2 flux is interannual variability in net air-sea CO_2 flux in all pixels for which NCP_{N2fix} values were available. We addressed this issue using multiannual pCO_2 climatology provided by Landschützer et al. (2014). For the ocean areas in which nC_T reduction occurred in the absence of N, interannual variability in the net air-sea CO_2 flux was estimated to be ±0.06 Pg C/year (1σ) for the period 1998–2011. The magnitude of this flux variability may be an error in our NCP_{N2fix} estimates arising from the net air-sea CO_2 flux and is comparable with the pCO_2 interpolation error reported by Takahashi et al. (2009) for the pCO_2 climatology.

In summary, the probable error in the estimated NCP_{N2fix} because of all sources of error was ±0.2 Pg C per 8 months.

4. Discussion

4.1. Factors Influencing NCP_{N2fix} Occurred During Periods of N Depletion

The NCP_{N2fix}, estimated by integrating the reduction in mixed layer C_T over the 8-month period of N depletion, potentially includes NCP contributed by sources other than N_2 fixation. To exclusively attribute our NCP_{N2fix} to N_2 fixation, it is necessary to evaluate other contributions. One of these is utilization of DON by non-N_2 fixing microorganisms during photosynthesis. This possibility is difficult to assess because the comparable DON utilization has yet to be reported (Church et al., 2002; Johnson et al., 2010; Karl et al., 2003), and consequently, we cannot discount this process as an alternative explanation because seawater DON data are not adequate to assess this explanation.

Lateral transport of N from the N-rich gyre margins added nutrients to the gyres from which much of our NCP_{N2fix} was derived. As noted in section 2, the flux ratio of C_T and NO_3^- to the subtropical gyre is a key measure in determining the impact of lateral N transport on NCP_{N2fix} in oligotrophic gyres. The C:N ratio in waters intruding from the gyre margins was greater than 7, except in the South Pacific Ocean (Letscher et al., 2016).

The slight elevation of the C:N ratio (relative to the Redfield value) for the intrusion waters indicates that our NCP_{N2fix} values for all basins other than the South Pacific were only slightly underestimated, because the C_T remained after the complete consumption of N would have offset our NCP_{N2fix} estimate. However, such offsets would have been minor.

Another biological process that could affect the NCP_{N2fix} occurring in the N-depleted ocean is selective N mining via vertical migration of phytoplankton. The results of a recent study indicate that in the N-limited ocean the diatom *Rhizosolenia* changes buoyancy to descend to the nitracline to acquire NO_3^- then returns to the surface to carry out photosynthesis. This N mining mechanism could transfer significant amounts of NO_3^- from depth (1–79.9 mmol N·m^{-2}·year^{-1}; Villareal et al., 2014). As much as 80 mmol N·m^{-2}·year^{-1} (equivalent to a total NCP of 0.56 mol C·m^{-2}·year^{-1}, half of the rate we estimated at the HOT station) could be similarly mined below the HOT station (Johnson et al., 2010). In contrast to all established physical mechanisms that simultaneously bring N and C from depth to the surface, this newly identified process mines only NO_3^- from the nitracline. The global significance of this process in the N budget of the upper ocean is difficult to assess because of the limited research currently undertaken (Johnson et al., 2010).

The above evaluation shows that it is not possible to unequivocally assign the contributions of alternative processes to our estimate of NCP_{N2fix} occurring in oceans where the levels of NO_3^- are below 0.2 μmol/kg.

4.2. Comparisons of NCP_{N2fix} at the HOT and BATS Stations and the South Pacific Ocean

Of the possible explanations for our estimate of NCP_{N2fix}, a major process is considered to be marine N_2 fixation, which generally occurs at a high rate in warm waters lacking N. To compare our estimate with measurements of the N_2 fixation rate, a C:N ratio of 7 was used to convert the rates of N_2 fixation to those of NCP_{N2fix}. Based on the $^{15}N_2$ assimilation method, the rate of N_2 fixation at the HOT station, averaged over the period of June 2005–December 2013, was 0.56 mol C·m^{-2}·year^{-1} (Böttjer et al., 2017), which is only half our rate estimated for a pixel that includes the HOT station (Figure 2a). However, the $^{15}N_2$-based rates of NCP_{N2fix} are comparable with our estimate, given that underestimation is an inherent problem associated with the ^{15}N-based method, which measures the net N_2 fixation rate rather than the gross rate (Böttjer et al., 2017; Mulholland, 2007; Wilson et al., 2012).

In contrast, the rates measured at the BATS station are only 6% of our estimate and do not fall within the uncertainty bracket of our estimate (Figure 2b). The rates reported at the BATS station were based on the earlier erroneous method (incomplete $^{15}N_2$ equilibrium) and thus may have underestimated the true rate of N_2 fixation by a factor of 2 or more (Großkopf et al., 2012). Another explanation for measurements being considerably lower at the BATS station than our C_T-based estimate is that the ^{15}N-based measurements at this station were designed to assess the contribution from *Trichodesmium* only (Orcutt et al., 2001). The difference between the ^{15}N-based estimates and our estimate may arise from large errors in assessments of the abundance of N_2 fixing organisms, associated with use of a conventional net sampling method. Application of an in situ digital microscope indicated a *Trichodesmium* abundance fourfold greater than that determined using the net sampling method (Davis & McGillicuddy, 2006). If these two sources of error are considered, the revised rate could be as high as 0.8 mol C·m^{-2}·year^{-1} (an eightfold increase). Moreover, the rates based on field measurements directed solely at *Trichodesmium* could be also underestimated because N_2 fixation is not limited to this cyanobacterium; other unicellular cyanobacteria in the ocean may contribute significantly to the N budget (Moisander et al., 2010; Thompson et al., 2012).

For the area defined by 20–30°S and 100–120°W in the South Pacific, our NCP_{N2fix} estimate (0.8 mol C/m^2 per 8 months) was comparable to the value (0.4 mol C/m^2 per 4 months; i.e., 0.8 mol C/m^2 if scaled up for 8 months of the warming period) derived from the winter-summer mixed layer C_T difference (Bender & Jönsson, 2016). The congruence of estimates based on these two methods supports the accuracy of our method. In contrast, Knapp et al. (2016) reported a low N_2 fixation rate (a maximum of approximately 100 μmol N·m^{-2}·day^{-1}, which is equivalent to 0.25 mol C/m^2 per 8 months) in the same area. One source of error in our NCP_{N2fix} estimate may have been lateral intrusion of N-rich water (C:N ratio < 7), which could have resulted in overestimation of the NCP_{N2fix}. The difference may also have arisen from errors in direct measurements based on the incomplete equilibrium of $^{15}N_2$ gas, which can result in underestimation of

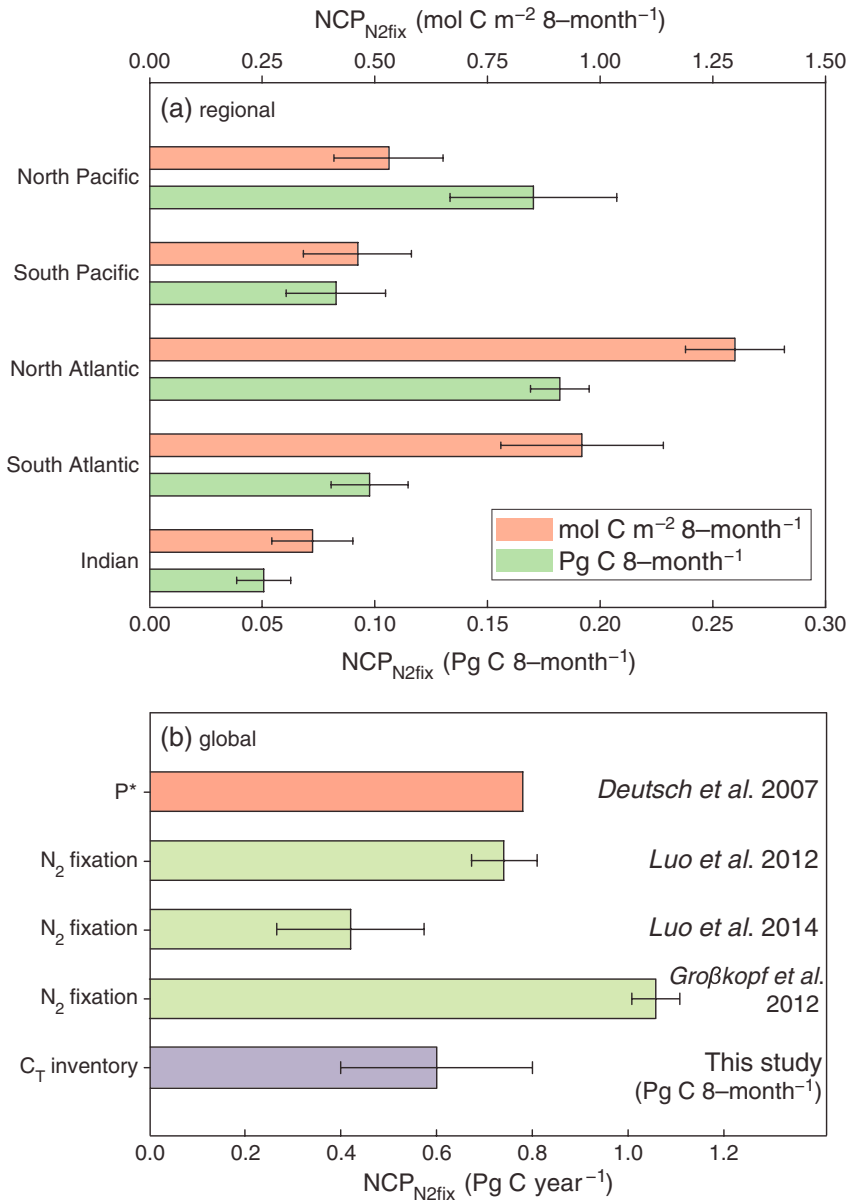

Figure 4. Comparison of (a) regional and (b) global NCP_{N2fix} in nitrate-depleted warm waters. Comparison of the rate of NCP_{N2fix} over the warming period (approximately 8 months), estimated in this study, with the annual rates estimated using measurements of the N_2 fixation rate and geochemical methods. We assumed an elemental C:N ratio of 7 to convert the marine N_2 fixation rate to NCP_{N2fix}. The error bar for our estimate was obtained from uncertainties associated with all terms in equation (1). NCP = net community production.

the N_2 fixation rate by 40–60%. These sources of error may collectively have contributed to differences in the NCP_{N2fix} estimates for the South Pacific based on our method and the ^{15}N-based method.

4.3. Global Comparisons of NCP_{N2fix}

Our NCP_{N2fix} value of 0.6 ± 0.2 Pg C per 8 months falls within the range of 0.3–1.0 Pg C/year, which has been derived from extrapolation of shipboard N_2 fixation measurements to the global ocean (Großkopf et al., 2012; Luo et al., 2012, 2014; Figure 4). However, regional- and basin-scale comparisons are not appropriate because most field measurements have been heavily biased toward the Atlantic Ocean.

The P^* method in conjunction with inverse modeling also yielded a comparable rate of 0.79 Pg C/year for NCP_{N2fix} supported by N_2 fixing microorganisms (Deutsch et al., 2007). However, differences are apparent

in regional comparisons. For example, the P^* method yielded the highest rate in the eastern Pacific Ocean, where N is abundant because of equatorial upwelling, and the P^* values are also highest. In contrast, our method did not calculate the NCP_{N2fix} for this area, because in this area the N concentration is high throughout the year. Another area of contrast is the Southern Ocean, where the P^* method yielded a considerable level of NCP_{N2fix} supported by N_2 fixers, but our method did not indicate any NCP_{N2fix}.

Comparison of our NCP_{N2fix} values with those obtained in other studies depends on the C:N ratio chosen to represent the value for dissolved and particulate organic matter produced by marine N_2 fixers. The elemental C:N ratio of 7 that we used for conversion of N_2 fixation rates to NCP_{N2fix} appears to be consistent with the values directly measured for *Trichodesmium* biomass but is much lower than the ratios (20–30) measured for semilabile dissolved organic matter produced largely by N_2 fixers (Church et al., 2002; Mulholland, 2007). The large variations among reported elemental C:N ratios are another source of uncertainty in estimates of N_2-supported NCP derived from direct measurements and indirect geochemical methods.

Much of the NCP_{N2fix} we calculated occurred in waters where the supply of iron and phosphate, which are limiting elements for N_2 fixation, is sufficient to support diazotrophs (Ward et al., 2013). During the warming period, when C_T declined in the absence of N, the seasonal reduction in PO_4^{3-} was also observed within the mixed layer of the ocean. The total PO_4^{3-} reduction yielded a NCP_{N2fix} (Data Set S2) of 0.3 Pg C per 8 months (Figure S2) using the C:P ratio of 195:1 representing particulate organic matter collected from the N-depleted ocean (Martiny et al., 2013). The PO_4^{3-}-based NCP_{N2fix} rate is approximately half of the C_T-based rate we determined. The difference between these rates may be insignificant given the large uncertainty (a factor of 4 greater than 195) in the C:P ratio of organic matter produced by N_2 fixing organisms.

5. Conclusions and Implication

The proposed method provides the global-scale NCP_{N2fix} of 0.6 ± 0.2 Pg C per 8 months in the vast areas of the N-depleted ocean, where NCP_{N2fix} cannot be accurately estimated using conventional methods for N_2 fixation activity. Our estimate represents NCP_{N2fix} that occurred during the warming period (approximately 8 months) and thus is certainly low, as our value does not include N_2-fixer-derived NCP during the cooling period as well as that which occurred in coastal waters.

The key requirement that NCP_{N2fix} can play a direct role in oceanic uptake of anthropogenic CO_2 is if it can change with future climate variations (Falkowski, 1997). A growing number of experiments and modeling studies pointed to the enhancement of the growth of N_2-fixing diazotrophs under high pCO_2 conditions (Dutkiewicz et al., 2015). This finding further suggests that NCP_{N2fix} in the vast areas of the N-depleted ocean gyre could be increased as a result of the enhancement of N_2 fixation activity, thus providing a negative feedback to the ocean carbon cycle. Ultimately, N_2 fixation will be limited by the availability of phosphate, iron, and other trace nutrients.

Acknowledgments
We are indebted to two anonymous referees for their comments, which greatly improved our error estimates. All data used in this analysis can be accessed from links provided in section 2 of the manuscript. This work was supported by Global Research Laboratory Program (2013K1A1A2A02078278) of the National Research Foundation of Korea (NRF) funded by the Ministry of Science, ICT and Future Planning. Additional support was provided by Mid-career Researcher Program (2018R1A2A1A19019281) of NRF, by *Management of Marine Organisms causing Ecological Disturbance and Harmful Effects* funded by the Ministry of Ocean and Fisheries (MOF), by *Ieodo Ocean Research Station* project of the Korea Hydrographic and Oceanographic Agency, MOF, and by *Isabu project* (PE99584) of Korean Institute of Ocean Science and Technology. Partial support was also provided by the Gordon and Betty Moore Foundation (award 3794 to D. M. K.) and by the Simons Foundation (SCOPE award 329108 to D. M. K.), by a grant from U.S. National Oceanic and Atmospheric Administration (NA150AR4320064, T. T.), and by MOF (20160245 PM18040) and Korea-Arctic Ocean Observing System (SHK).

References

Antonov, J., Seidov, D., Boyer, T., Locarnini, R., Mishonov, A., Garcia, H., et al. (2010). In S. Levitus (Ed.), *World Ocean Atlas 2009, Volume 2: Salinity*, NOAA Atlas NESDIS (Vol. 69, 184 pp.). Washington, DC: U.S. Government Printing Office. https://www.nodc.noaa.gov/OC5/WOA09/woa09data.html

Bender, M. L., & Jönsson, B. (2016). Is seasonal net community production in the South Pacific subtropical gyre anomalously low? *Geophysical Research Letters*, *43*, 9757–9763. https://doi.org/10.1002/2016GL070220

Böttjer, D., Dore, J. E., Karl, D. M., Letelier, R. M., Mahaffey, C., Wilson, S. T., et al. (2017). Temporal variability of nitrogen fixation and particulate nitrogen export at Station ALOHA. *Limnology and Oceanography*, *62*(1), 200–216. https://doi.org/10.1002/lno.10386

Capone, D. G., Zehr, J. P., Paerl, H. W., Bergman, B., & Carpenter, E. J. (1997). *Trichodesmium*, a globally significant marine cyanobacterium. *Science*, *276*(5316), 1221–1229. https://doi.org/10.1126/science.276.5316.1221

Church, M. J., Ducklow, H. W., & Karl, D. M. (2002). Multiyear increases in dissolved organic matter inventories at Station ALOHA in the North Pacific Subtropical Gyre. *Limnology and Oceanography*, *47*(1), 1–10. https://doi.org/10.4319/lo.2002.47.1.0001

Davis, C. S., & McGillicuddy, D. J. (2006). Transatlantic abundance of the N_2-fixing colonial cyanobacterium *Trichodesmium*. *Science*, *312*(5779), 1517–1520. https://doi.org/10.1126/science.1123570

de Boyer Montégut, C., Madec, G., Fischer, A. S., Lazar, A., & Iudicone, D. (2004). Mixed layer depth over the global ocean: An examination of profile data and a profile-based climatology. *Journal of Geophysical Research*, *109*, C12003. https://doi.org/10.1029/2004JC002378

Deutsch, C., Sarmiento, J. L., Sigman, D. M., Gruber, N., & Dunne, J. P. (2007). Spatial coupling of nitrogen inputs and losses in the ocean. *Nature*, *445*(7124), 163–167. https://doi.org/10.1038/nature05392

Dickson, A. (1990). Thermodynamics of the dissociation of boric acid in synthetic seawater from 273.15 to 318.15 K. *Deep Sea Research Part A. Oceanographic Research Papers*, *37*(5), 755–766. https://doi.org/10.1016/0198-0149(90)90004-F

Dickson, A., & Millero, F. (1987). A comparison of the equilibrium constants for the dissociation of carbonic acid in seawater media. *Deep Sea Research Part A. Oceanographic Research Papers*, *34*(10), 1733–1743. https://doi.org/10.1016/0198-0149(87)90021-5

Duce, R., LaRoche, J., Altieri, K., Arrigo, K., Baker, A., Capone, D., et al. (2008). Impacts of atmospheric anthropogenic nitrogen on the open ocean. *Science*, *320*(5878), 893–897. https://doi.org/10.1126/science.1150369

Dutkiewicz, S., Morris, J. J., Follows, M. J., Scott, J., Levitan, O., Dyhrman, S. T., & Berman-Frank, I. (2015). Impact of ocean acidification on the structure of future phytoplankton communities. *Nature Climate Change*, *5*(11), 1002–1006. https://doi.org/10.1038/nclimate2722

Falkowski, P. G. (1997). Evolution of the nitrogen cycle and its influence on the biological sequestration of CO_2 in the ocean. *Nature*, *387*(6630), 272–275. https://doi.org/10.1038/387272a0

Galloway, J. N., Dentener, F. J., Capone, D. G., Boyer, E. W., Howarth, R. W., Seitzinger, S. P., et al. (2004). Nitrogen cycles: Past, present, and future. *Biogeochemistry*, *70*(2), 153–226. https://doi.org/10.1007/s10533-004-0370-0

Garcia, H., Locarnini, R., Boyer, T., Antonov, J., Baranova, O., Zweng, M., et al. (2014). In S. Levitus (Ed.), *World Ocean Atlas 2013, Volume 4: Dissolved Inorganic Nutrients (Phosphate, Nitrate, Silicate)*, *NOAA Atlas NESDIS* (Vol. 76, p. 25). Washington, DC: U.S. Government Printing Office. https://www.nodc.noaa.gov/OC5/woa13/

Großkopf, T., Mohr, W., Baustian, T., Schunck, H., Gill, D., Kuypers, M. M., et al. (2012). Doubling of marine dinitrogen–fixation rates based on direct measurements. *Nature*, *488*(7411), 361–364. https://doi.org/10.1038/nature11338

Gruber, N. (2016). Elusive marine nitrogen fixation. *Proceedings of the National Academy of Sciences of the USA*, *113*(16), 4246–4248. https://doi.org/10.1073/pnas.1603646113

Gruber, N., & Galloway, J. N. (2008). An Earth-system perspective of the global nitrogen cycle. *Nature*, *451*(7176), 293–296. https://doi.org/10.1038/nature06592

Gruber, N., Keeling, C. D., & Stocker, T. F. (1998). Carbon-13 constraints on the seasonal inorganic carbon budget at the BATS station in the northwestern Sargasso Sea. *Deep Sea Research Part I: Oceanographic Research Papers*, *45*(4-5), 673–717. https://doi.org/10.1016/S0967-0637(97)00098-8

Gruber, N., & Sarmiento, J. L. (1997). Global patterns of marine nitrogen fixation and denitrification. *Global Biogeochemical Cycles*, *11*(2), 235–266. https://doi.org/10.1029/97GB00077

Hood, R. R., Coles, V. J., & Capone, D. G. (2004). Modeling the distribution of *Trichodesmium* and nitrogen fixation in the Atlantic Ocean. *Journal of Geophysical Research*, *109*, C06006. https://doi.org/10.1029/2002JC001753

Hood, R. R., Michaels, A. F., & Capone, D. G. (2000). Answers sought to the enigma of marine nitrogen fixation. *Eos, Transactions American Geophysical Union*, *81*(13), 133–139. https://doi.org/10.1029/00EO00086

Johnson, K. S., Riser, S. C., & Karl, D. M. (2010). Nitrate supply from deep to near-surface waters of the North Pacific subtropical gyre. *Nature*, *465*(7301), 1062–1065. https://doi.org/10.1038/nature09170

Karl, D. M., Bates, N. R., Emerson, S., Harrison, P. J., Jeandel, C., Llinâs, O., et al. (2003). Temporal studies of biogeochemical processes determined from ocean time-series observations during the JGOFS era. In M. J. R. Fasham (Ed.), *Ocean biogeochemistry: The role of the ocean carbon cycle in global change* (pp. 239–267). Berlin, Heidelberg: Springer. https://doi.org/10.1007/978-3-642-55844-3_11

Karl, D. M., Michaels, A., Bergman, B., Capone, D., Carpenter, E., Letelier, R., et al. (2002). Dinitrogen fixation in the world's oceans. *Biogeochemistry*, *57*(1), 47–98. https://doi.org/10.1023/A:1015798105851

Kavanaugh, M. T., Church, M. J., Davis, C. O., Karl, D. M., Letelier, R. M., & Doney, S. C. (2018). ALOHA from the edge: Reconciling three decades of in situ Eulerian observations and geographic variability in the North Pacific Subtropical Gyre. *Frontiers in Marine Science*, *5*(130). https://doi.org/10.3389/fmars.2018.00130

Kim, D. O., Lee, K., Choi, S. D., Kang, H. S., Zhang, J. Z., & Chang, Y. S. (2005). Determination of diapycnal diffusion rates in the upper thermocline in the North Atlantic Ocean using sulfur hexafluoride. *Journal of Geophysical Research*, *110*, C10010. https://doi.org/10.1029/2004JC002835

Kim, I.-N., Lee, K., Gruber, N., Karl, D. M., Bullister, J. L., Yang, S., & Kim, T.-W. (2014). Increasing anthropogenic nitrogen in the North Pacific Ocean. *Science*, *346*(6213), 1102–1106. https://doi.org/10.1126/science.1258396

Kim, T.-W., Lee, K., Najjar, R. G., Jeong, H.-D., & Jeong, H. J. (2011). Increasing N abundance in the northwestern Pacific Ocean due to atmospheric nitrogen deposition. *Science*, *334*(6055), 505–509. https://doi.org/10.1126/science.1206583

Knapp, A. N., Casciotti, K. L., Berelson, W. M., Prokopenko, M. G., & Capone, D. G. (2016). Low rates of nitrogen fixation in eastern tropical South Pacific surface waters. *Proceedings of the National Academy of Sciences of the USA*, *113*(16), 4398–4403. https://doi.org/10.1073/pnas.1515641113

Lamarque, J.-F., Dentener, F., McConnell, J., Ro, C., Shaw, M., Vet, R., et al. (2013). Multi-model mean nitrogen and sulfur deposition from the Atmospheric Chemistry and Climate Model Intercomparison Project (ACCMIP): Evaluation historical and projected changes. *Atmospheric Chemistry and Physics*, *13*(16), 7997–8018. https://doi.org/10.5194/acp-13-7997-2013

Landschützer, P., Gruber, N., Bakker, D. C. E., & Schuster, U. (2014). Recent variability of the global ocean carbon sink. *Global Biogeochemical Cycles*, *28*, 927–949. https://doi.org/10.1002/2014GB004853

Ledwell, J. R., Watson, A. J., & Law, C. S. (1998). Mixing of a tracer in the pycnocline. *Journal of Geophysical Research*, *103*(C10), 21,499–21,529. https://doi.org/10.1029/98JC01738

Lee, K. (2001). Global net community production estimated from the annual cycle of surface water total dissolved inorganic carbon. *Limnology and Oceanography*, *46*(6), 1287–1297. https://doi.org/10.4319/lo.2001.46.6.1287

Lee, K., Karl, D. M., Wanninkhof, R., & Zhang, J. Z. (2002). Global estimates of net carbon production in the nitrate-depleted tropical and subtropical oceans. *Geophysical Research Letters*, *29*(19), 1907. https://doi.org/10.1029/2001GL014198

Lee, K., Kim, T.-W., Byrne, R. H., Millero, F. J., Feely, R. A., & Liu, Y.-M. (2010). The universal ratio of boron to chlorinity for the North Pacific and North Atlantic oceans. *Geochimica et Cosmochimica Acta*, *74*(6), 1801–1811. https://doi.org/10.1016/j.gca.2009.12.027

Lee, K., Millero, F. J., Byrne, R. H., Feely, R. A., & Wanninkhof, R. (2000). The recommended dissociation constants for carbonic acid in seawater. *Geophysical Research Letters*, *27*(2), 229–232. https://doi.org/10.1029/1999GL002345

Lee, K., Millero, F. J., & Campbell, D. M. (1996). The reliability of the thermodynamic constants for the dissociation of carbonic acid in seawater. *Marine Chemistry*, *55*(3), 233–245. https://doi.org/10.1016/S0304-4203(96)00064-3

Lee, K., Tong, L. T., Millero, F. J., Sabine, C. L., Dickson, A. G., Goyet, C., et al. (2006). Global relationships of total alkalinity with salinity and temperature in surface waters of the world's oceans. *Geophysical Research Letters*, *33*, L19605. https://doi.org/10.1029/2006GL027207

Lee, K., Wanninkhof, R., Feely, R. A., Millero, F. J., & Peng, T. H. (2000). Global relationships of total inorganic carbon with temperature and nitrate in surface seawater. *Global Biogeochemical Cycles*, *14*(3), 979–994. https://doi.org/10.1029/1998GB001087

Letscher, R. T., Primeau, F., & Moore, J. K. (2016). Nutrient budgets in the subtropical ocean gyres dominated by lateral transport. *Nature Geoscience*, *9*(11), 815–819. https://doi.org/10.1038/ngeo2812

Lomas, M. W., Bates, N. R., Johnson, R. J., Knap, A. H., Steinberg, D. K., & Carlson, C. A. (2013). Two decades and counting: 24-years of sustained open ocean biogeochemical measurements in the Sargasso Sea. *Deep Sea Research Part II: Topical Studies in Oceanography*, *93*, 16–32. https://doi.org/10.1016/j.dsr2.2013.01.008

Luo, Y.-W., Doney, S. C., Anderson, L. A., Benavides, M., Berman-Frank, I., Bode, A., et al. (2012). Database of diazotrophs in global ocean: Abundance, biomass and nitrogen fixation rates. *Earth System Science Data*, *4*(1), 47–73. https://doi.org/10.5194/essd-4-47-2012

Luo, Y.-W., Lima, I. D., Karl, D. M., Deutsch, C. A., Doney, S. C., et al. (2014). Data-based assessment of environmental controls on global marine nitrogen fixation. *Biogeosciences*, *11*(3), 691–708. https://doi.org/10.5194/bg-11-691-2014

Martiny, A. C., Pham, C. T., Primeau, F. W., Vrugt, J. A., Moore, J. K., Levin, S. A., & Lomas, M. W. (2013). Strong latitudinal patterns in the elemental ratios of marine plankton and organic matter. *Nature Geoscience*, *6*(4), 279–283. https://doi.org/10.1038/ngeo1757

McGillicuddy, D. J., Anderson, L. A., Bates, N. R., Bibby, T., Buesseler, K. O., Carlson, C. A., et al. (2007). Eddy/wind interactions stimulate extraordinary mid-ocean plankton blooms. *Science*, *316*(5827), 1021–1026. https://doi.org/10.1126/science.1136256

McGillicuddy, D. J., Robinson, A. R., Siegel, D. A., Jannasch, H. W., Johnson, R., Dickey, T. D., et al. (1998). Influence of mesoscale eddies on new production in the Sargasso Sea. *Nature*, *394*(6690), 263–266. https://doi.org/10.1038/28367

Mehrbach, C., Culberson, C., Hawley, J., & Pytkowicx, R. (1973). Measurement of the apparent dissociation constants of carbonic acid in seawater at atmospheric pressure. *Limnology and Oceanography*, *18*(6), 897–907. https://doi.org/10.4319/lo.1973.18.6.0897

Michaels, A. F., Bates, N. R., Buesseler, K. O., Carlson, C. A., & Knap, A. H. (1994). Carbon-cycle imbalances in the Sargasso Sea. *Nature*, *372*(6506), 537–540. https://doi.org/10.1038/372537a0

Moisander, P. H., Beinart, R. A., Hewson, I., White, A. E., Johnson, K. S., Carlson, C. A., et al. (2010). Unicellular cyanobacterial distributions broaden the oceanic N_2 fixation domain. *Science*, *327*(5972), 1512–1514. https://doi.org/10.1126/science.1185468

Mulholland, M. R. (2007). The fate of nitrogen fixed by diazotrophs in the ocean. *Biogeosciences*, *4*(1), 37–51. https://doi.org/10.5194/bg-4-37-2007

Olsen, A., Key, R. M., van Heuven, S., Lauvset, S. K., Velo, A., Lin, X., et al. (2016). The Global Ocean Data Analysis Project version 2 (GLODAPv2)-an internally consistent data product for the world ocean. *Earth System Science Data*, *8*(2), 297–323. https://doi.org/10.5194/essd-8-297-2016

Orcutt, K. M., Lipschultz, F., Gundersen, K., Arimoto, R., Michaels, A. F., Knap, A. H., & Gallon, J. R. (2001). A seasonal study of the significance of N_2 fixation by *Trichodesmium* spp. at the Bermuda Atlantic time-series study (BATS) station. *Deep Sea Research Part II: Topical Studies in Oceanography*, *48*(8-9), 1583–1608. https://doi.org/10.1016/S0967-0645(00)00157-0

Pidcock, R. E., Martin, A. P., Painter, S., Allen, J. T., Srokosz, M. A., Forryan, A., et al. (2016). Quantifying mesoscale-driven nitrate supply: A case study. *Global Biogeochemical Cycles*, *30*, 1206–1223. https://doi.org/10.1002/2016GB005383

Quay, P., & Stutsman, J. (2003). Surface layer carbon budget for the subtropical N. Pacific: $\delta^{13}C$ constraints at station ALOHA. *Deep Sea Research Part I: Oceanographic Research Papers*, *50*(9), 1045–1061. https://doi.org/10.1016/S0967-0637(03)00116-X

Raes, E. J., Thompson, P. A., McInnes, A. S., Nguyen, H. M., Hardman-Mountford, N., & Waite, A. M. (2015). Sources of new nitrogen in the Indian Ocean. *Global Biogeochemical Cycles*, *29*, 1283–1297. https://doi.org/10.1002/2015GB005194

Sudre, J., Maes, C., & Garçon, V. (2013). On the global estimates of geostrophic and Ekman surface currents. *Limnology and Oceanography: Fluids and Environments*, *3*(1), 1–20. https://doi.org/10.1215/21573689-2071927

Takahashi, T., Sutherland, S., Chipman, D., Goddard, J., Ho, C., Newberger, T., et al. (2014). Climatological distributions of pH, pCO_2, total CO_2, alkalinity, and $CaCO_3$ saturation in the global surface ocean, and temporal changes at selected locations. *Marine Chemistry*, *164*, 95–125. https://doi.org/10.1016/j.marchem.2014.06.004

Takahashi, T., Sutherland, S. C., Wanninkhof, R., Sweeney, C., Feely, R. A., Chipman, D. W., et al. (2009). Climatological mean and decadal change in surface ocean pCO_2, and net sea-air CO_2 flux over the global oceans. *Deep Sea Research Part II: Topical Studies in Oceanography*, *56*(8-10), 554–577. https://doi.org/10.1016/j.dsr2.2008.12.009

Thompson, A. W., Foster, R. A., Krupke, A., Carter, B. J., Musat, N., Vaulot, D., et al. (2012). Unicellular cyanobacterium symbiotic with a single-celled eukaryotic alga. *Science*, *337*(6101), 1546–1550. https://doi.org/10.1126/science.1222700

Villareal, T. A., Pilskaln, C. H., Montoya, J. P., & Dennett, M. (2014). Upward nitrate transport by phytoplankton in oceanic waters: Balancing nutrient budgets in oligotrophic seas. *PeerJ*, *2*, e302. https://doi.org/10.7717/peerj.302

Ward, B. A., Dutkiewicz, S., Moore, C. M., & Follows, M. J. (2013). Iron, phosphorus, and nitrogen supply ratios define the biogeography of nitrogen fixation. *Limnology and Oceanography*, *58*(6), 2059–2075. https://doi.org/10.4319/lo.2013.58.6.2059

Weiss, R. F. (1974). Carbon dioxide in water and seawater: The solubility of a non–ideal gas. *Marine Chemistry*, *62*(1), 200–216. https://doi.org/10.1016/0304-4203(74)90015-2

Wilson, S. T., Böttjer, D., Church, M. J., & Karl, D. M. (2012). Comparative assessment of nitrogen fixation methodologies, conducted in the oligotrophic North Pacific Ocean. *Applied and Environmental Microbiology*, *78*(18), 6516–6523. https://doi.org/10.1128/AEM.01146-12

Yao, W., & Millero, F. J. (1995). The chemistry of the anoxic waters in the Framvaren Fjord, Norway. *Aquatic Geochemistry*, *1*(1), 53–88. https://doi.org/10.1007/BF01025231

Yasunaka, S., Ono, T., Nojiri, Y., Whitney, F. A., Wada, C., Murata, A., et al. (2016). Long-term variability of surface nutrient concentrations in the North Pacific. *Geophysical Research Letters*, *43*(7), 3389–3397. https://doi.org/10.1002/2016GL068097

Zhang, J. Z., Wanninkhof, R., & Lee, K. (2001). Enhanced new production observed from the diurnal cycle of nitrate in an oligotrophic anticyclonic eddy. *Geophysical Research Letters*, *28*(8), 1579–1582. https://doi.org/10.1029/2000GL012065